ARTICLES

One- and Two-Photon Photosensitized Singlet Oxygen Production: Characterization of Aromatic Ketones as Sensitizer Standards

Jacob Arnbjerg,[†] Martin J. Paterson,[†,‡] Christian B. Nielsen,[†,§] Mikkel Jørgensen,[§] Ove Christiansen,[†] and Peter R. Ogilby*[,†]

Department of Chemistry, University of Aarhus, DK-8000 Århus, Denmark, Risø National Laboratory, Frederiksborgvej 399, DK-4000 Roskilde, Denmark, and School of Engineering and Physical Sciences, Heriot-Watt University, Edinburgh EH14 4AS, Scotland

Received: February 12, 2007; In Final Form: May 1, 2007

Singlet molecular oxygen, $O_2(a^1\Delta_g)$, can be efficiently produced in a photosensitized process using either one- or two-photon irradiation. The aromatic ketone 1-phenalenone (PN) is an established one-photon singlet oxygen sensitizer with many desirable attributes for use as a standard. In the present work, photophysical properties of two other aromatic ketones, pyrene-1,6-dione (PD) and benzo[*cd*]pyren-5-one (BP), are reported and compared to those of PN. Both PD and BP sensitize the production of singlet oxygen with near unit quantum efficiency in a nonpolar (toluene) and a polar (acetonitrile) solvent. With their more extensive π networks, the one-photon absorption spectra for PD and BP extend out to longer wavelengths than that for PN, thus providing increased flexibility for sensitizer excitation over the range ∼300−520 nm. Moreover, PD and BP have much larger two-photon absorption cross sections than PN over the range 655−840 nm which, in turn, results in amounts of singlet oxygen that are readily detected in optical experiments. One- and two-photon absorption spectra of PD and BP obtained using high-level calculations model the salient features of the experimental data well. In particular, the ramifications of molecular symmetry are clearly reflected in both the experimental and calculated spectra. The use of PD and BP as standards for both the one- and two-photon photosensitized production of singlet oxygen is expected to facilitate the development of new sensitizers for application in singlet-oxygen-based imaging experiments.

Introduction

The first excited electronic state of molecular oxygen, singlet oxygen, $O_2(a^1\Delta_g)$, is a reactive species that can mediate the oxidative degradation of many molecules.[1] These reactions can have important ramifications in a host of polymeric as well as biological systems.[2] Of particular significance are the roles played by singlet oxygen in mechanisms of cell signaling and cell death.[3] The latter forms the basis for photodynamic therapy, PDT, a medical procedure used to destroy unwanted tissue (*e.g.*, cancerous tumors).[4]

For most practical purposes, singlet oxygen is conveniently generated in a photosensitized process wherein a molecule (*i.e.*, the sensitizer) absorbs light and subsequently transfers a fraction of this excitation energy to ground state oxygen, $O_2(X^3\Sigma_g^-)$, to form singlet oxygen (Figure 1).[5] It is generally implied that the photosensitized production of singlet oxygen proceeds via the absorption of a single photon that is sufficiently energetic to populate an excited electronic state of the sensitizer (*e.g.*, the lowest excited singlet state, S_1; see Figure 1). Although energy transfer to ground state oxygen can occur from S_1, quenching of a longer-lived sensitizer triplet state by oxygen is generally most efficient.[5] As a consequence, desirable singlet oxygen sensitizers generally have large quantum yields of S → T intersystem crossing (Figure 1). Over the past ∼40 years, a large number of molecules have been identified and characterized as singlet oxygen sensitizers upon one-photon excitation in the UV, visible, and near IR regions of the spectrum.[6]

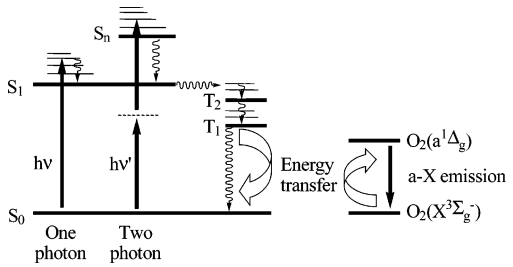

Figure 1. Schematic illustration of the one- and two-photon photosensitized production of singlet oxygen. The weak near IR radiative transition, $O_2(a^1\Delta_g) \rightarrow O_2(X^3\Sigma_g^-)$ phosphorescence, commonly used to detect singlet oxygen is also shown.

It has recently been shown that singlet oxygen can also be produced upon two-photon excitation of a sensitizer.[7−12] In this process, two comparatively low-energy photons are simultaneously absorbed to populate a sensitizer excited state (Figure 1). Depending on the molecule, this state can be different than S_1 (*vide infra*). Two-photon absorption is a nonlinear process in which the extent of excited-state population increases

* To whom correspondence should be addressed. E-mail: progilby@chem.au.dk.
[†] University of Aarhus.
[‡] Heriot-Watt University.
[§] Risø National Laboratory.

10.1021/jp071197l CCC: $37.00
Published on Web 06/12/2007

CHART 1: Molecules Examined in the Present Study[a]

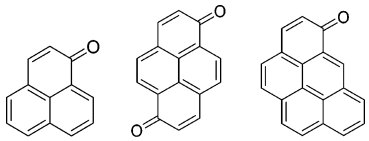

PN (C_s) **PD (C_{2h})** **BP (C_s)**

[a] PN: 1-phenalenone. PD: pyrene-1,6-dione. BP: benzo[*cd*]pyren-5-one. The corresponding molecular point groups are shown in parentheses.

quadratically with an increase in the intensity of the incident light. This has the desirable attribute that, when using a focused laser beam as the irradiating source, sensitizer excitation and hence singlet oxygen production can be confined to a comparatively small volume.[13,14] This feature of sensitizer excitation can have important ramifications in optical imaging experiments based on the near IR phosphorescence of singlet oxygen or simply in experiments in which one wants to control the spatial domain in which singlet oxygen is produced.[14,15]

Over the last ~5 years, an increasing amount of information has been compiled in the characterization of two-photon singlet oxygen sensitizers.[7−12,16,17] Such information includes correlations between the structure of a given molecule and the spectral profile for two-photon absorption, the probability for two-photon absorption as expressed through the so-called two-photon absorption cross section (δ), singlet oxygen quantum yields (Φ_Δ), and stability upon prolonged irradiation. These data are clearly a prerequisite in the design and development of efficient two-photon sensitizers for specific purposes, such as selective imaging agents for biological systems.[13−15]

The development and characterization of singlet oxygen sensitizers is greatly simplified when one has a standard molecule against which one can compare certain measurable quantities. Two quantities that are particularly pertinent in this regard are the singlet oxygen quantum yield, Φ_Δ, and the wavelength-dependent two-photon absorption cross section, δ, both of which are readily obtained in experiments that rely on the use of a calibrated standard.[6,18] Such standards should clearly have well-defined and accurate values of Φ_Δ and δ. The standard should also be reasonably stable upon prolonged irradiation and should have one- and two-photon absorption profiles conducive to irradiation over a broad spectral range.

Aromatic ketones such as benzanthrone, 4-phenylbenzophenone, and dibenzopyrenequinone are generally known to be efficient singlet oxygen sensitizers.[6,19] One aromatic ketone that has been studied extensively and that is now often used as a standard sensitizer for one-photon excitation is 1-phenalenone, PN (Chart 1, also sometimes called perinaphthenone).[19−22] This molecule has the particularly desirable feature of producing singlet oxygen with near unit quantum efficiency in a wide range of solvents.[21] Although the PN absorption spectrum has a band maximum around 355 nm, which conveniently corresponds to a commonly used laser wavelength (*i.e.*, the third harmonic of a Nd:YAG laser), the absence of appreciable PN absorption at wavelengths longer than ~420 nm can limit the use of this molecule as a one-photon standard. To our knowledge, the two-photon absorption properties of PN have previously not been examined.

To establish a more encompassing series of singlet oxygen sensitizers based on the successful aromatic ketone motif exemplified in PN, we first set forth to characterize the two-photon absorption properties of PN. We then embarked on a project to synthesize and characterize other aromatic ketones based on the PN motif but with extended conjugation and/or additional carbonyl functionalities. The intent in the development of these new molecules was to create a sensitizer system that could be used over a wider spectral range. Moreover, we wanted to capitalize on the concept that an extended π network is generally conducive to the creation of large transition moments which, in turn, should enhance two-photon absorption cross sections.[23−25] Finally, through the judicious placement on the molecule of an additional carbonyl group, we could address the extent to which symmetry influences one- and two-photon transitions, respectively. The aromatic ketones chosen for this study, pyrene-1,6-dione (PD) and benzo[*cd*]pyren-5-one (BP), are also shown in Chart 1.

To complement our experimental studies, we also set out to examine aspects of our molecules using computations performed at a comparatively high level of theory. Specifically, significant improvements in the calculation of two-photon absorption cross sections and transition energies have become possible due to advances in response theory, and this newer methodology has been successfully applied to molecular systems as large as those shown in Chart 1.[8,17,26−28] Although the features of response theory are described elsewhere,[29−33] it is pertinent to note here that response theory implicitly sums over all states in the system without explicitly constructing these states. This is particularly important for the problem at hand, because the two-photon transition proceeds by a virtual state (dashed line in Figure 1) which is a linear combination of all real eigenstates in the system. Response theory complements state-of-the-art electronic structure methods including density functional theory (DFT) and coupled cluster theory.[34,35] Thus, increasingly accurate theories can be applied to nonlinear optical problems and this has been substantiated, for example, in recent comparisons of results obtained using higher-order density functional response theory with those obtained using high-level coupled cluster methods (*e.g.*, CC3 quadratic response).[36] The successful application of such theories to molecules as large as those used in the present study is currently one of the challenges in the field.

Experimental Section

One-Photon Instrumentation and Methods. One-photon absorption spectra were recorded using a Hewlett-Packard/Agilent model 8453 diode array spectrometer, whereas fluorescence spectra and quantum yields were measured using a Horiba Jobin Yvon fluorometer (Fluoromax P). Fluorescence quantum yields were determined using 9,10-dicyanoanthracene in toluene as a standard [Φ_F(N_2 saturated solution) = 0.76 ± 0.03,[37] Φ_F(air- saturated solution) = 0.69 ± 0.05[38]].

In one series of experiments, singlet oxygen quantum yields, Φ_Δ, were determined upon nanosecond irradiation of the sensitizer using the 355 nm third harmonic of a Nd:YAG laser (Quanta Ray GCR 230). These measurements were performed using two independent and complementary techniques: (1) In a time-resolved optical experiment, the amount of singlet oxygen produced was quantified by recording the 1270 nm $O_2(a^1\Delta_g) \rightarrow O_2(X^3\Sigma_g^-)$ phosphorescence intensity. Values for the phosphorescence intensity were obtained by extrapolating the time-resolved signal to zero time, and recording such data over a wide range of incident laser powers.[39] Corresponding data were recorded from PN, which was used as a reference standard with Φ_Δ = 0.98 ± 0.05 (see discussion in text). Experiments were performed in air-saturated solutions. Pertinent data are provided in the Supporting Information. (2) Time-resolved laser-induced optoacoustic calorimetric (LIOAC) measurements were used to indirectly quantify the amount of singlet oxygen produced. In

TABLE 1: Calculated Vertical Excitation Energies, One-Photon Oscillator Strengths, and Two-Photon Absorption Cross Sections, δ, for PD Using Three Different Basis Sets

One-Photon Transitions

	cc-pVDZ		aug-cc-pVDZ		cc-pVTZ	
state	E (eV)	oscillator strength[a]	E (eV)	oscillator strength[a]	E (eV)	oscillator strength[a]
1 B_u	3.11	0.341	3.02	0.338	3.05	0.333
1 A_u	3.10	0.000	3.12	0.000	3.13	0.000
2 B_u	3.73	0.090	3.66	0.101	3.67	0.095
3 B_u	5.01	0.000	4.92	0.002	4.95	0.001
4 B_u	5.49	0.326	5.37	0.332	5.42	0.329
2 A_u	5.76	0.000	5.76	0.000	5.78	0.000
3 A_u	6.05	0.000	5.99	0.000	6.04	0.000
4 A_u	6.67	0.000	6.09	0.004	6.66	0.000

Two-Photon Transitions[b]

	cc-pVDZ		aug-cc-pVDZ		cc-pVTZ	
state	E (eV)	δ (au)	E (eV)	δ (au)	E (eV)	δ (au)
1 B_g	2.96	0.011	2.99	0.005	2.99	0.007
1 A_g	3.43	881.4	3.34	913.3	3.37	863.6
2 A_g	4.97	9806	4.92	13271	4.94	11257
3 A_g	5.46	3391	5.35	5761	5.41	4651
4 A_g	5.58	642.2	5.44	779.0	5.49	386.3
2 B_g	5.59	3.53	5.55	9.73	5.56	7.32
3 B_g	5.68	6.35	5.64	4.22	5.64	3.84
4 B_g	6.00	5.90	5.97	7.53	5.99	4.10

[a] Dipole length gauge (*i.e.*, dipole moment operators in terms of *x*, *y*, and *z* position coordinates). [b] Linearly parallel polarized photons of equal energy (*i.e.*, at half eigenstate energy).

this case, optoacoustic waveforms resulting from nonradiative heat emission from excited states of the sensitizer can be used to infer the singlet oxygen yield.[19,21,40] Experiments were performed in oxygen-saturated solutions. Independent LIOAC experiments were also performed in the absence of oxygen to determine sensitizer triplet state energies. In all cases, optoacoustic waveform amplitudes in the LIOAC experiments were measured relative to a standard, 2-hydroxybenzophenone (2-HBP), which, independent of oxygen concentration in non-H-bonding solvents, releases all its excitation energy as heat within $\sim$35 ps.[41]

In separate time-resolved optical experiments where Φ_Δ was quantified using the singlet oxygen phosphorescence intensity, PD and BP were irradiated at 416 nm. This latter wavelength was obtained through stimulated Raman scattering in H_2 gas of the 355 nm third harmonic output of the Nd:YAG laser (416 nm is the first Stokes line). The details of this technique employed for the present experiments are similar to those we have employed in the past,[42] with the exception that our laser now has a filled-Gaussian spatial mode pattern. The standard sensitizer used for these experiments was 2,5-dibromo-1,4-bis-(2-(4-(diphenylamino)phenyl)vinyl)benzene, BrPhVB, which produces singlet oxygen with a quantum yield of 0.45 $\pm$ 0.05. (In earlier experiments,[10] a value of Φ_Δ(BrPhVB) = 0.46 $\pm$ 0.05 was determined against Φ_Δ(PN) = 1.00 $\pm$ 0.05 as a standard. The present value of Φ_Δ(BrPhVB) = 0.45 $\pm$ 0.05 reflects our use of Φ_Δ(PN) = 0.98 $\pm$ 0.05 as a standard.) In reporting the Φ_Δ data in Table 2, the results of the 416 nm experiments are distinguished from those obtained in the 355 nm experiments.

The singlet oxygen phosphorescence experiments were typically performed using laser energies over the range $\sim$50$-$400 μJ/pulse with the laser operating at a repetition rate of 10 Hz and a beam diameter in the sample of $\sim$3$-$4 mm. This corresponds to average laser powers over the range 0.5$-$4.0 mW. The LIOAC experiments were performed using laser energies over the range $\sim$5$-$40 μJ/pulse, but with a beam diameter of $\sim$1 mm (the latter facilitates a reduction in the acoustic transit time, τ_a; see text).

Triplet absorption measurements to determine sensitizer triplet state lifetimes were likewise recorded using instruments that have been previously described.[7] Although triplet absorption spectra were not explicitly recorded, measurements were performed at a wavelength between 400 and 600 nm where the amplitude of the transient signal was the largest. The lowest energy triplet state of PN, for example, is known to absorb in this spectral region.[20]

Two-Photon Instrumentation and Methods. The femtosecond excitation source and optical detection apparatus used to record two-photon excitation spectra are described in detail elsewhere.[8,10] Briefly, we used a Ti:sapphire laser system (Spectra Physics, Tsunami and Spitfire) that delivers femtosecond pulses at a repetition rate of 1 kHz that are tunable over the range $\sim$765$-$850 nm. Generation of excitation wavelengths outside this spectral range is achieved by pumping an optical parametric amplifier (Spectra Physics, OPA-800CF), resulting in linearly polarized, femtosecond pulses tunable over the range $\sim$300$-$3000 nm.

The sensitizer solution was contained in a 1 cm path length cuvette, and sample luminescence was detected by a cooled VIS/near-IR sensitive photomultiplier tube, PMT (Hamamatsu model R5509-42). Because the spectral response of the PMT covers the range $\sim$400$-$1500 nm, either $O_2(a^1\Delta_g)$ phosphorescence centered at 1270 nm or visible fluorescence from our two-photon standards could be readily monitored by using appropriate interference and band-pass filters. The output of the PMT was amplified (Stanford Research Systems model 445 preamplifier) and sent to a photon counter (Stanford Research Systems model 400) operated using a program written in LabView (National Instruments, Inc.).

Two-photon excitation spectra for the aromatic ketones were obtained using the phosphorescence of singlet oxygen as a spectroscopic probe. The details of this approach are likewise presented elsewhere.[8,10] Data were recorded in increments of 10$-$15 nm, which corresponds to the approximate spectral width of our femtosecond excitation pulses.[8] In these experiments, the effects of wavelength-dependent changes in the temporal and spatial profiles of the pulsed laser were incorporated as outlined below by simultaneously recording data from a standard molecule whose two-photon absorption spectrum has been corrected for these variables. Two-photon absorption cross sections for PD, BP, and PN at a given wavelength, $\delta(\lambda)$, were obtained using eq 1. Here the subscript *r* refers to the reference compound, and *S*, *P*, *C*, and Φ_Δ are the observed two-photon signal, irradiation power at the sample, sensitizer concentration, and singlet oxygen quantum yield, respectively.

$$\delta(\lambda) = \frac{S(\lambda)\Phi_{\Delta,r}C_rP_r^2}{S_r(\lambda)\Phi_\Delta CP^2}\delta_r(\lambda) \quad (1)$$

The reference standard used was 2,5-dicyano-1,4-bis(2-(4-(diphenylamino)phenyl)vinyl)benzene, denoted CNPhVB (Φ_Δ = 0.11 $\pm$ 0.02).[10,43] The two-photon absorption spectrum of CNPhVB in toluene over the range 730$-$900 nm has been published,[8] whereas the spectrum over the range 625$-$730 nm was determined in the current study. This was done in an independent fluorescence excitation experiment performed against 1,4-bis(2-methylstyryl)benzene, denoted bis-MSB, dissolved in cyclohexane for which the two-photon spectral profile

TABLE 2: Summary of Photophysical Parameters for the Sensitizers PN, PD, and BP

sens	solvent	E_S (kJ/mol)	E_T (kJ/mol)	α	Φ_Δ[a]	δ (GM)[b]
PN	toluene	~265[c]	181 ± 12	0.73 ± 0.02[d] 0.48 ± 0.02[e]	0.97 ± 0.06[f]	6.5 ± 1 @ 685 nm
PD	toluene	253 ± 3	146 ± 10	0.73 ± 0.02[d] 0.58 ± 0.02[e]	0.97 ± 0.06[f] 0.95 ± 0.05[g] 0.98 ± 0.11[g] (416 nm)	59 ± 8 @ 655 nm
	CH_3CN				1.01 ± 0.05[g]	
BP	toluene	237 ± 3	145 ± 10	0.72 ± 0.02[d] 0.57 ± 0.02[e]	1.00 ± 0.06[f] 0.96 ± 0.05[g] 1.03 ± 0.12[g] (416 nm)	29 ± 6 @ 655 nm
	CH_3CN				0.92 ± 0.06[g]	

[a] Irradiation wavelength was 355 nm, except where otherwise indicated. [b] 1 GM = 10^{-50} cm^4 s photon^{-1}. [c] Reference 21. [d] Oxygen-saturated. [e] Nitrogen-saturated. [f] LIOAC. [g] Singlet oxygen phosphorescence.

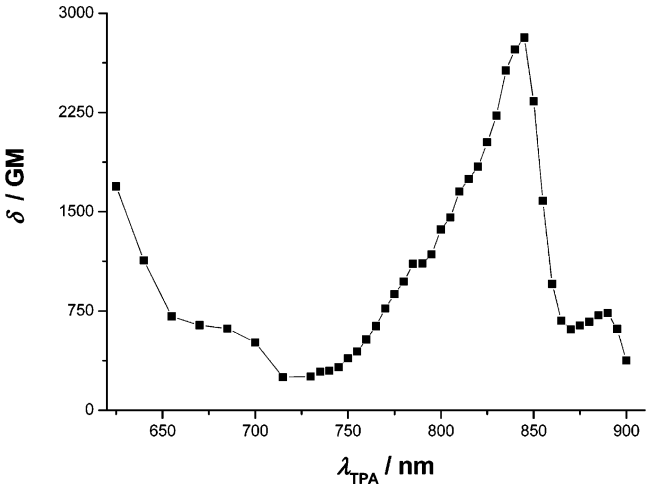

Figure 2. Two-photon absorption spectrum for CNPhVB in toluene.

over the range 537−780 nm has been established.[44,45] For this independent study, eq 1 was simply modified by replacing values of Φ_Δ with values for the quantum yield of fluorescence, Φ_F. The fluorescence of bis-MSB was monitored at 440 nm ($\Phi_F = 0.98$[46]), whereas CNPhVB fluorescence was monitored at 520 nm ($\Phi_F = 0.86 \pm 0.07$[47]). It is important to note that this relative experiment against bis-MSB was used only to yield the spectral profile of CNPhVB; the scale for the two-photon absorption cross section, δ, was established using the existing CNPhVB data at 730 nm (*i.e.*, the common point between the old and new experiments). At wavelengths shorter than 625 nm, the intensity of the observed CNPhVB fluorescence signal deviated from the required power-squared dependence and approached a linear dependence indicating that, at these shorter wavelengths, one-photon absorption competes with two-photon absorption. The resultant two-photon absorption spectrum of CNPhVB used as the standard for the singlet oxygen experiments over the range 625−900 nm is shown in Figure 2.

All two-photon experiments on PN, PD, and BP were performed using toluene as the solvent. We have previously demonstrated that absorption by toluene itself can provide complications in a two-photon experiment.[10,17] Nevertheless, for the present study, we ascertained that at each excitation wavelength used, absorption by the solvent does not interfere with the data obtained.

Materials and Sample Preparation. The di-ketone PD was prepared according to the procedure reported by Fatiadi[48] and BP was prepared according to the procedure reported by Reid and Bonthrone.[49] NMR spectra for the latter compound, which, to our knowledge, have yet to be published, are provided in the Supporting Information. The syntheses for CNPhVB and BrPhVB are likewise presented elsewhere.[7] 1,4-Bis(2-methylstyryl)benzene, bis-MSB (>99.5%, Aldrich), and 2-HBP (99%, Aldrich) were used as received. Toluene, cyclohexane, acetonitrile, and methanol were all spectroscopic grade (Aldrich) and used as received. Deoxygenated samples were prepared by gently bubbling the solution with solvent-saturated, dry nitrogen for 25 min.

For the data shown in Table 2, PN (97%, Aldrich) was used as received. However, in an independent series of control experiments, we established that data recorded using this commercial-grade PN were indistinguishable from data recorded using PN that had been recrystallized. The data obtained in these control experiments and the details of PN recrystallization are provided in the Supporting Information.

Computational Details

Ground state geometries were optimized using density functional theory (DFT) with the B3LYP functional and the cc-pVDZ basis set, as implemented in the Gaussian program.[50] The harmonic vibrational frequencies calculated from the second derivatives at each critical point confirmed that minima were obtained.

At the minimum energy geometries, we computed both one- and two-photon absorption spectra using density functional response theory as implemented in a local version of the Dalton program.[51] We used the CAM-B3LYP functional as this has been shown to give reliable two-photon results compared to high accuracy coupled-cluster response calculations.[36] In comparison to the B3LYP functional, use of the CAM-B3LYP functional results in a better description of excited states mainly due to the increased flexibility in the exchange functional caused by "switching on" and increasing the amount of "exact" Hartree−Fock exchange into the Kohn−Sham orbitals as the interelectronic distance increases. This flexibility also improves the description of the intermediate (*i.e.*, virtual) states in the two-photon process which are a linear combination of excited states but that invariably have a different character than the excited state ultimately populated.[52]

In the response theory calculations, the one-photon spectra were obtained from the linear response function whereas the two-photon spectra were obtained from the quadratic response function, the poles giving the excitation energies and the residues the transition moments.[29] More specifically with respect to the latter, we obtain the spatially dependent components of the two-photon transition tensor T from the first residue of the quadratic response function.[29] To facilitate discussion it is sometimes convenient to describe these components of the tensor T in a sum-over-states expression such as that shown in eq 2.[26] In eq

$$T_{\alpha\beta} = \sum_j \frac{\langle 0|\mu_\alpha|j\rangle\langle j|\mu_\beta|\mathrm{f}\rangle}{\omega_j - \omega} + \frac{\langle 0|\mu_\beta|j\rangle\langle j|\mu_\alpha|\mathrm{f}\rangle}{\omega_j - \omega} \qquad (2)$$

2, T is expressed in terms of the transition moments between ground, 0, intermediate or virtual, j, and final, f, states, where ω_j denotes the excitation frequency of the jth state, ω the

frequency of the irradiating light, and μ_α and μ_β are the spatially dependent components of the electric dipole operator (*i.e.*, α and β refer to the Cartesian coordinates *x*, *y*, and *z*).[53−56] Note that the summation is carried over all intermediate states *j*, including the ground state. However, it is important to stress that eq 2 is not required in the response calculation, and that the summation over all states *j* is implicit in the value of *T* obtained through the response calculation.

Calculated values of *T* can then be used to obtain the two-photon absorption cross section, δ. As shown in eq 3, the latter is reported as a rotationally averaged quantity

$$\delta = \frac{F}{30}\sum_{\alpha,\beta} T_{\alpha\alpha}T^*_{\beta\beta} + \frac{G}{30}\sum_{\alpha,\beta} T_{\alpha\beta}T^*_{\alpha\beta} + \frac{H}{30}\sum_{\alpha,\beta} T_{\alpha\beta}T^*_{\beta\alpha} \quad (3)$$

and *F*, *G*, and *H* depend on the polarization of the incident photons.[53,54,57] Under our conditions in which excitation is achieved using linearly polarized light, $F = G = H = 2$. The two-photon calculations were carried out with identical photon energies equal to half the vertical excitation energy of the final state, a condition consistent with the experiments that were performed.

The calculated two-photon absorption cross sections are reported in atomic units (au), not in the so-called Göppert-Mayer units (GM) pertinent to experimental results (1 GM = 10^{-50} cm^4 s $photon^{-1}$). (Note: In expressing this unit, $photon^{-1}$ is occasionally omitted.) A more complete discussion of the conversion from atomic units to GM is presented elsewhere.[26] In this conversion, it is pertinent to note that the lifetime dependent broadening of the excited quantum levels is sometimes treated phenomenologically in the expression for the absorption cross section through the inclusion of a band shape function.[26,27,54,58−60] Although some attempts have been made to include molecule specific band shape functions,[26] the use of a constant, molecule-independent multiplicative scaling factor is commonly employed.[58,59] In the present work, we have chosen not to include such functions or scaling factors, and we report our results in atomic units.

Basis Sets. The use of large and diffuse basis functions is sometimes necessary in the computation of certain molecular properties, particularly those that depend on excited-state character.[30,61] It has been shown that even multiple sets of diffuse functions may be required (*e.g.*, with quantitative coupled-cluster calculations of two-photon absorption cross sections for small molecules).[36] DFT is generally less sensitive to the quality of the basis set than correlated *ab initio* methods.[62] However, the importance of diffuse functions in higher-order density functional response theory is not well established. It is known that in the DFT-based calculation of nonlinear hyperpolarizabilities on small molecules, diffuse functions are essential but that as the chromophore becomes larger the importance of such functions is expected to diminish.[63] Because both the first hyperpolarizabilty and two-photon absorption cross section are derived from the quadratic response function, one may expect a similar situation for two-photon calculations.

Therefore, in an independent exercise, we set out to investigate the importance of both the size and nature of the basis set used in the response calculations on one of our comparatively large molecules. This exercise complements our earlier benchmark studies on the computation of nonlinear optical properties in small molecules.[36,60] In the present study, we obtained excitation energies, one-photon oscillator strengths, and two-photon absorption cross sections for PD in three separate calculations using the basis sets cc-pVDZ, aug-cc-pVDZ, and cc-pVTZ, respectively. The results of these calculations are shown in Table 1.

As can be seen in Table 1, the inclusion of diffuse functions in going from cc-pVDZ to aug-cc-pVDZ, as well as the increase in the valence basis in going from cc-pVDZ to the significantly larger set cc-pVTZ has an effect on excitation energies, one-photon oscillator strengths, and two-photon absorption cross sections for PD. Despite these changes, the overall pictures that evolve using these basis sets are nevertheless very similar. Of course, proper treatment of Rydberg states requires diffuse functions in the basis set. Indeed, as we proceed to the higher energy transitions in Table 1, we see larger differences in the results obtained with the respective basis sets. Nevertheless, such differences are only appreciable in states whose energies exceed ~5.5 eV which, at least, is outside the energy range pertinent for the present experimental study on PD, BP, and PN.

Thus, the key conclusion of this independent exercise is that we observe no significant changes in the parameters calculated as a function of the basis set used. More specifically, the basis-set-dependent changes in the parameters calculated using density functional response methods for PD are smaller than the corresponding changes observed in our previous study on small molecules using both DFT and wavefunction-based response methodologies.[36] The fact that, when working with large molecules, one can use even the simple cc-pVDZ basis set and still achieve a reasonable result is important. The use of such a basis set provides computational savings not just with respect to the shear number of functions handled, but also with regards to the convergence of the DFT equations. With the results of this independent study in mind, we nevertheless used the cc-pVTZ basis set for all subsequent calculations presented in this report.

Of course, it is also pertinent to note that, for the present study, the calculations are performed on gas-phase systems that lack solvent-dependent perturbations. Moreover, the effects of molecular vibrations and vibronic coupling are not taken into account. As such, comparisons to our solution-phase experimental data must be considered in light of these additional sources of uncertainty, and we must focus only on general qualitative trends in the comparison between experimental and computational data.

Results and Discussion

A. One-Photon Properties.

A.1. Optical Characterization.

A.1.a. Spectroscopy. One-photon absorption spectra for PD, BP, and PN in toluene are shown in Figure 3a. On the basis solely of changes in the structure of the three molecules, we expect a bathochromic shift upon going from PN to PD to BP because additional conjugation is successively introduced in the respective chromophores. This is indeed the case, as illustrated in Figure 3a, rendering PD and BP suitable for excitation beyond the long wavelength absorption limit of PN. Also, in comparison with PN, both PD and BP exhibit larger molar extinction coefficients, ϵ, in the longest wavelength absorption band.

The one-photon spectrum of PN has been studied and discussed extensively,[20−22,64] and many features of this discussion can be applied directly to PD and BP. Due to its relatively large ϵ value, the PN absorption band with a maximum at 358 nm in toluene has been assigned to a $\pi \rightarrow \pi^*$ transition.[20,21] Similarly, we assign the PD band with a maximum at 432 nm and the BP band with a maximum at 468 nm to $\pi \rightarrow \pi^*$ transitions. All of these assignments are consistent with the results obtained from our calculations (*vide infra*, Table 3).

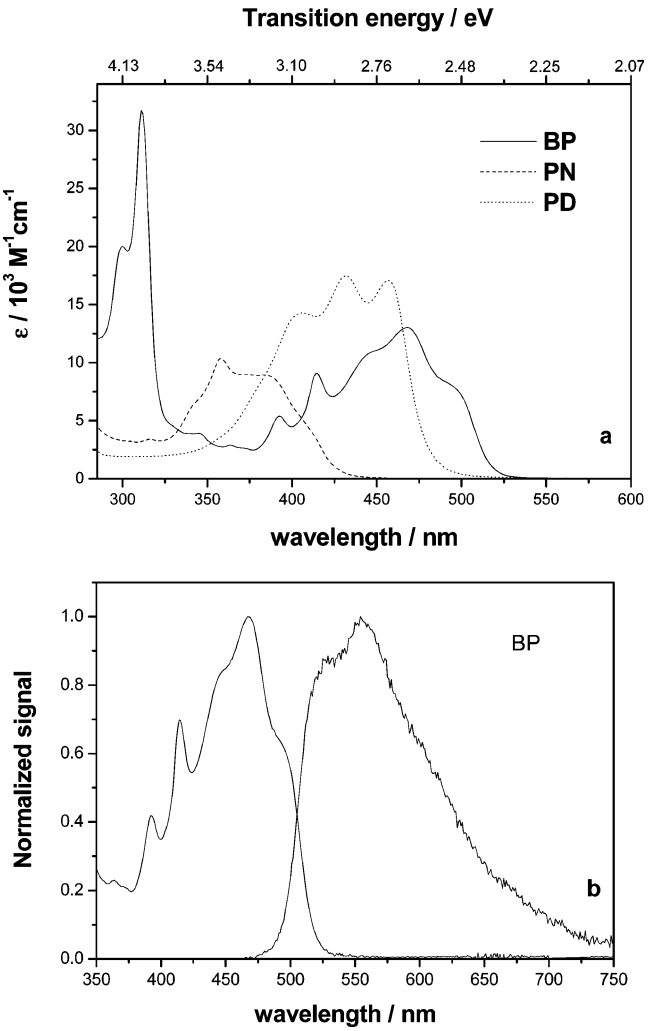

Figure 3. (a) Absorption spectra for PN, PD and BP in toluene. The *x*-axis in electron volts is included to facilitate comparison with data in Table 3. (b) Absorption and fluorescence spectra for BP in toluene.

TABLE 3: Calculated Vertical Excitation Energies, One-Photon Oscillator Strengths and Two-Photon Absorption Cross Sections, δ, for Transitions in PN, PD, and BP[a]

state	character	energy (eV)	one-photon oscillator strength[b]	two-photon absorption cross section[c]
		PD (C_{2h})		
1 B_g	$n_A\pi^*$[d]	2.99	0.000	0.007
1 B_u	$\pi\pi^*$	3.05	0.333	0.000
1 A_u	$n_S\pi^*$[d]	3.13	0.000	0.000
1 A_g	$\pi\pi^*$	3.37	0.000	863.6
2 B_u	$\pi\pi^*$	3.67	0.095	0.000
2 A_g	$\pi\pi^*$	4.94	0.000	11257
3 B_u	$\pi\pi^*$	4.95	0.001	0.000
3 A_g	$\pi\pi^*$	5.41	0.000	4651
4 B_u	$\pi\pi^*$	5.42	0.329	0.000
4 A_g	$\pi\pi^*$	5.49	0.000	386.3
		BP (C_s)		
1 A′	$\pi\pi^*$	3.01	0.284	240.5
1 A″	$n\pi^*$	3.22	0.000	0.001
2 A′	$\pi\pi^*$	3.61	0.038	96.7
3 A′	$\pi\pi^*$	4.11	0.038	697.9
4 A′	$\pi\pi^*$	4.50	0.158	372.5
5 A′	$\pi\pi^*$	4.61	0.286	295.3
6 A′	$\pi\pi^*$	4.62	0.015	2623
		PN (C_s)		
1 A″	$n\pi^*$	3.30	0.000	0.001
1 A′	$\pi\pi^*$	3.57	0.206	55.9
2 A′	$\pi\pi^*$	4.07	0.050	46.3
3 A′	$\pi\pi^*$	4.51	0.032	274.1
4 A′	$\pi\pi^*$	5.35	0.259	492.7

[a] Response calculations performed with the CAM-B3LYP functional and the cc-pVTZ basis set. [b] Length gauge (*i.e.*, dipole moment operators in terms of *x*, *y* and *z* position coordinates). [c] Rotationally averaged value, calculated using linearly parallel polarized photons. Reported in atomic units (au), not GM (see manuscript text). [d] n_S refers to the in-plane combination of oxygen lone-pair orbitals that is symmetric with respect to the principal C_2 symmetry axis, whereas n_A refers to the combination of orbitals that is antisymmetric with respect to this axis.

With respect to our calculations in Table 3, we find that the energy difference between the lowest π,π^* and n,π^* singlet states is comparatively small for all three molecules. Moreover, this difference is arguably smaller than the errors of our calculation. Nevertheless, we find that the lowest energy singlet states in both PN and PD are n,π^* states. Although S_1 in BP is calculated to be of π,π^* character, the n,π^* state is sufficiently close in energy that state mixing will likely add some n,π^* character to S_1 here as well (again, recall that our calculations do not consider the effects of vibronic coupling and solvent perturbation). It is important to note, however, that for all three molecules, we calculate a one-photon oscillator strength of effectively zero for the transitions in which the n,π^* state is populated. For PN, these results are consistent with experimental data; to our knowledge, a weak transition to the n,π^* state has been observed in only one solvent, cyclohexane.[21] Otherwise, the absorption spectroscopy of these aromatic ketones is dominated by $\pi \rightarrow \pi^*$ transitions.

A dominant $\pi \rightarrow \pi^*$ transition with a band maximum at 311 nm is also seen in the spectrum of BP and reflects population of a higher-energy state S_n (Figure 3a, Table 3). In toluene, the corresponding transition could not be observed for PN and PD due to absorption by the solvent. However, upon dissolving PN and PD in methanol, the UV bands were observed (see Supporting Information). These latter spectra reveal a band maximum of 248 nm with $\epsilon \sim 19\,800$ M^{-1} cm^{-1} for PN and a band maximum of 209 nm with $\epsilon \sim 49\,400$ M^{-1} cm^{-1} for PD (our spectrum for PN in methanol is similar to a spectrum recorded in acetonitrile[64]).

In both toluene and acetonitrile, PN, PD, and BP are weakly fluorescent. In toluene, BP has a fluorescence quantum yield, Φ_F, of 0.004, whereas PN and PD have fluorescence quantum yields smaller than 0.0001. In all cases, the fluorescence signals observed were independent of whether the experiment was performed in an air- or nitrogen-saturated solution, indicating that oxygen does not quench S_1 in these molecules. The weak fluorescence is attributed to the carbonyl in the chromophore, which facilitates efficient intersystem crossing from the singlet into the triplet manifold (see discussion below about triplet yields). Despite this weak fluorescence, we were nevertheless able to use the point at which the scaled fluorescence and absorption spectra intersect (*e.g.*, Figure 3b) to estimate the singlet energies for PD and BP: $E_S(\text{PD}) = 253 \pm 3$ and $E_S(\text{BP}) = 237 \pm 3$ kJ/mol (Note: Given the procedure, these numbers are an estimate of the 0,0 energy.) For PN, an E_S value of ~265 kJ/mol has been reported on the basis of absorption spectra recorded in cyclohexane and acetonitrile.[21]

A.1.b. Singlet Oxygen Quantum Yields. Quantum yields of singlet oxygen production, Φ_Δ, for PD and BP were obtained by monitoring the relative intensities of the time-resolved singlet oxygen phosphorescence signals upon one-photon excitation of the sensitizer. These experiments were performed using two different excitation wavelengths. In one study, excitation was

at 355 nm. The standard sensitizer used in this case was PN, for which we have used $\Phi_\Delta = 0.98 \pm 0.05$ for experiments performed in toluene and acetonitrile. This latter value of Φ_Δ is consistent with published data[21] as well as our own independent LIOAC measurement (*vide infra*, Table 2). The use of $\Phi_\Delta(\mathrm{PN}) = 0.98 \pm 0.05$ is likewise consistent with the common practice of using $\Phi_\Delta(\mathrm{PN}) = 1.0$. In a second study, performed in toluene, excitation was at 416 nm. The standard sensitizer used in this case was BrPhVB, which has a Φ_Δ value of 0.45 ± 0.05 (see Experimental Section). Through these experiments we found that, within the cited errors, PD and BP produce singlet oxygen with quantum yields that are essentially unity in both solvents (Table 2). Moreover, we confirmed that the lifetimes obtained from the time-resolved signals were ~30 μs in toluene and ~80 μs in acetonitrile, which are in agreement with the accepted values of the singlet oxygen lifetime in these solvents.[5,65] Pertinent data from these quantum yield studies are provided in the Supporting Information.

The fact that the singlet oxygen quantum yield is independent of excitation wavelength affirms that Kasha's rule indeed holds for these compounds. Specifically, irrespective of which state is initially populated, rapid internal conversion ensures that, for a given molecule, singlet oxygen production originates from a common state. This issue is certainly relevant in considering the two-photon photosensitized production of singlet oxygen where we likewise assume that, following the dictates of Kasha's rule, the immediate precursor to singlet oxygen is the same state as that produced upon one-photon excitation.[7]

A.1.c. Triplet Absorption Experiments. Triplet absorption experiments were performed on all three ketones in toluene. In these experiments, it was ascertained that the lifetime of the lowest energy triplet state, τ_T, is comparatively long in nitrogen-saturated solutions (*e.g.*, 370 ± 50 μs for PD). Of course, caution must be exercised in citing and interpreting such lifetimes simply because it is extremely difficult to ensure that all of the oxygen has indeed been removed from the system. Nevertheless, in air-saturated solutions, values of τ_T drop to a few hundred nanoseconds (*e.g.*, 300 ± 100 ns for PD). These observations are in agreement with previous studies on PN,[20,21] and indicate that, once produced in air-saturated toluene, greater than 99% of the ketone triplet states are quenched by ground state oxygen.

These oxygen quenching experiments also affirm that, in toluene, hydrogen atom abstraction from the solvent by the ketone triplet state is simply not a competitive reaction channel. Indeed, this conclusion is consistent with our assignment (*vide infra*) of π,π^* character to the lowest energy triplet states of these ketones (*i.e.*, as opposed to triplet states with n,π^* character, those with π,π^* character generally do not efficiently abstract hydrogen atoms[66]). This apparent absence of hydrogen abstraction reactions is also pertinent for affirming the validity of the LIOAC experiments discussed in the next section.

A.1.d. Sensitizer Stability. We ascertained that PD and BP showed no evidence of photoinduced degradation upon continuous irradiation for 20 min in air-saturated toluene using the 355 nm output of a Nd:YAG laser operated at a 10 Hz repetition rate. The extent of degradation, or rather the lack thereof, was assessed by looking for changes in the absorption spectrum of the molecule. The laser intensities used for this test were the same as the highest intensities used in our one-photon spectroscopic experiments (see experimental section).

A.2. Optoacoustic Characterization.

A.2.a. General Background. PN, PD, and BP are ideal molecules for characterization by laser-induced optoacoustic calorimetry, LIOAC. Application of LIOAC to study aromatic ketones, including PN, has previously been demonstrated,[19,21] and it is only necessary for us to summarize key points pertinent to our own discussion.

Briefly, upon laser irradiation of these essentially nonfluorescent molecules in a nitrogen-saturated solvent, the law of energy conservation results in eq 4,[40] where E_L is the molar

$$E_L(1 - \alpha) = \Phi_T E_T \exp(-\tau_T/\tau_a) \quad (4)$$

laser energy and α is the fraction of the excitation energy released as "fast" heat. With such aromatic ketones and in the absence of oxygen, the only energy storing state with an appreciable lifetime is the $v = 0$ level of the lowest triplet excited-state and, as such, the right-hand side of eq 4 is expressed as a function of the quantum yield, molar energy and lifetime (Φ_T, E_T and τ_T, respectively) of this triplet state.

The time scale pertinent for distinguishing "fast" and "slow" events is embodied in the effective acoustic transit time, τ_a, which is expressed in terms of the diameter, *d*, of the laser beam used for irradiation and v_a, the speed of sound in the sample ($\tau_a = d/v_a$). For the present experiment, $\tau_a \sim 1$ μs as determined by a Gaussian spatial beam profile with $d = 1.3$ mm and a speed of sound in toluene of $v_a = 1320$ m/s.[10] Compared with τ_a, the energy storing species is much longer lived (*i.e.*, $\tau_T \gg \tau_a$), whereas "fast" heat release as embodied in the parameter α reflects the nonradiative decay of species with lifetimes much shorter than τ_a. Molecular processes that contribute to α are internal conversion in the singlet manifold and intersystem crossing into the triplet manifold followed by internal conversion within this manifold.

Experimentally, α for a given compound can be found by measuring the maximum amplitudes, *H*, of optoacoustic waveforms obtained in a LIOAC experiment.[40] The value of α is then obtained through eq 5, where *A* is the sample absorbance

$$\alpha = H/(\kappa E_L(1 - 10^{-A})) \quad (5)$$

at the irradiation wavelength and κ is an instrumental constant. To avoid determining κ, experiments are performed relative to a calorimetric reference compound, for which the value of α is known.[40]

We used 2-hydroxybenzophenone (2-HBP) as a calorimetric reference for experiments performed in toluene. Under both oxygen- and nitrogen-saturated conditions in this solvent, 2-HBP converts all the excitation energy into heat within ~ 35 ps,[41] and, as such, has an α value of 1.0. Using eq 5, plots of $H/(1 - 10^{-A})$ versus E_L were generated in LIOAC experiments performed as a function of the incident laser energy (Figure 4). Values of α derived from these plots are given in Table 2.

It is important to recognize that, in a LIOAC experiment, the optoacoustic signal originates from photoinduced volume changes in the sample.[40] We have thus far implied that, in our experiments, such volume changes derive solely from radiationless transitions in the solute which result in the local heating of the solvent. In some cases, however, the LIOAC data also reflect photoinduced structural changes in the solute itself.[67−69] For the aromatic ketones examined in this study, we assume that such structural changes in the solute are either not pronounced and/or they do not significantly influence the optoacoustic signal recorded. A similar assumption has been made in analogous LIOAC studies of other aromatic ketones, including PN.[19] The validity of this assumption for PD and BP is affirmed through the fact that our independent optical data are essentially equivalent to our LIOAC data (Table 2, *vide infra*).

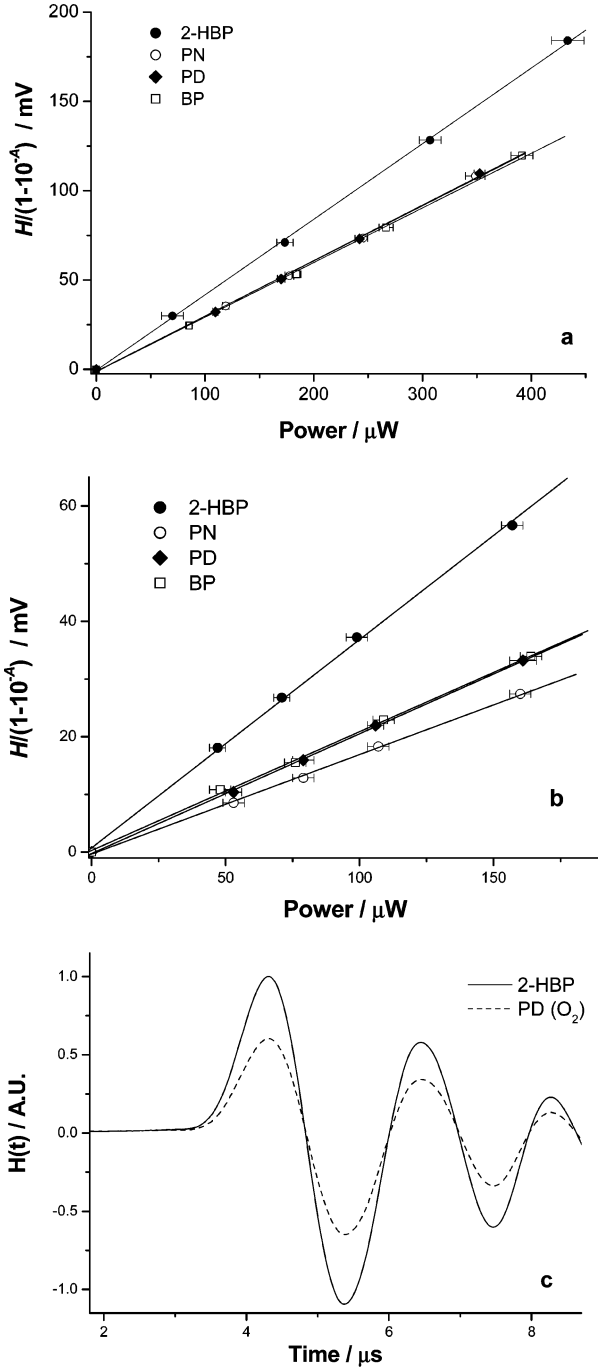

Figure 4. Observed LIOAC amplitudes, H, divided by $(1-10^{-A})$ and plotted against the average incident laser power for 2-HBP, PN, PD, and BP in toluene. Errors on values of $H/(1-10^{-A})$ are less than ~1% and thus, on this scale, are smaller than the symbol used to mark a given data point. (a) Oxygen-saturated conditions yielding values for α_{oxygen} and Φ_Δ. (b) Nitrogen-saturated conditions yielding values for $\alpha_{nitrogen}$ and E_T. As required by eq 5, all linear fits intercept at the origin. In panel c we show the time-resolved LIOAC waveforms recorded for both 2-HBP and PD under oxygen-saturated conditions. Note the absence of a phase shift between the respective traces. The latter is a prerequisite when using values of H to quantify Φ_Δ (see discussion in ref 19).

A.2.b. Singlet Oxygen Yields. We now consider LIOAC data recorded from oxygen-saturated solutions. From our triplet absorption studies, recall we ascertained that effectively all of the sensitizer triplet states produced upon irradiation are quenched by ground state oxygen and that the corresponding triplet state lifetime is in the nanosecond domain. As such, it should be clear that heat-releasing events related to the deactivation of the sensitizer triplet state are incorporated into α and that the only long-lived energy storing species must be singlet oxygen. Thus, under oxygen-saturated conditions, the energy conservation expression (eq 4) is written as a function of the quantum yield, molar energy, and lifetime of singlet oxygen (eq 6). Moreover, because the singlet oxygen lifetime, τ_Δ, is

$$E_L(1-\alpha) = \Phi_\Delta E_\Delta \exp(-\tau_\Delta/\tau_a) \qquad (6)$$

much longer than τ_a, the exponential term in eq 6 is effectively 1.0. Thus, eq 6 reduces to an expression for the singlet oxygen quantum yield, Φ_Δ (*i.e.*, $\Phi_\Delta = E_L(1-\alpha)/E_\Delta$), where E_Δ is the excitation energy of singlet oxygen (94 kJ/mol).

Values of Φ_Δ and α for PN, PD, and BP thus derived from the LIOAC experiment are listed in Table 2. It is seen that these Φ_Δ values are nearly identical to those obtained from the singlet oxygen phosphorescence experiments, confirming that these aromatic ketones indeed sensitize the production of singlet oxygen with near unit quantum efficiency in toluene. It is important to keep in mind that the LIOAC approach is based on experiments relative to 2-HBP, which is a molecule that does not produce singlet oxygen at all. This method is thus an independent verification that $\Phi_\Delta \sim 1$ for PN, the standard used in our phosphorescence experiments. We therefore conclude that the extended chromophores of PD and BP do not affect the production efficiency of singlet oxygen. These molecules are therefore highly suitable as one-photon standard singlet oxygen photosensitizers, with the additional desired feature that they complement the use of PN by extending the range of possible excitation wavelengths.

A.2.c. The Sensitizer Triplet State. From the observation that $\Phi_\Delta \sim 1$ for all three ketones, and given the reasonable assumption that oxygen does not quench the sensitizer singlet state (*i.e.*, S_1 is too short-lived), it immediately follows that the quantum yield of the sensitizer triplet state is also near unity (*i.e.*, $\Phi_T \sim \Phi_\Delta$, with errors that match those on our Φ_Δ values.). This result is consistent with our fluorescence data (*vide supra*) and strongly suggests that intersystem crossing into the triplet manifold is the sole fate of the S_1 state of these ketones. Indeed, such a conclusion is consistent with the extensive literature on the photophysics of aromatic ketones.[66]

For aromatic ketones in general,[5] and PN in particular,[20,64] it is well-established that the high singlet oxygen production efficiency in aprotic solvents is due to the fact that the pertinent energy donating state of the sensitizer, the T_1 state, has a π,π^* configuration. On this basis, we assume that this T_1 π,π^* orbital configuration also applies for PD and BP. These orbital configuration assignments for the respective triplet states are consistent with the results of our independent calculations (see Supporting Information). Although the $\pi \rightarrow \pi^*$ transitions are the most dominant in the singlet manifold, we have indicated that S_1 could still contain a certain amount of n,π^* character (*vide supra*, Table 3). This is particularly reasonable when a perturbation such as vibronic coupling can serve to mix states that are nearly degenerate. Of course, in accordance with El-Sayed's rules,[70] facile $S_1 \rightarrow T_1$ intersystem crossing will only occur for a transition between states with a different orbital configuration (*i.e.*, n,$\pi^* \leftrightarrow \pi,\pi^*$). Considering that the T_1 energy is substantially lower than that of S_1 for all three sensitizers (Table 2), $S_1 \rightarrow T_1$ intersystem crossing likely occurs through another higher energy triplet state (*e.g.*, T_2; see Figure 1). This higher energy triplet state could contain an appreciable amount of n,π^* character (see Supporting Information) and thus facilitate the $S_1 \rightarrow T_1$ conversion from an S_1 state with appreciable π,π^* character.

Knowing that $\Phi_T \sim \Phi_\Delta$ for these ketones, we can determine triplet state energies, E_T, by performing LIOAC experiments

in a nitrogen-saturated solvent. Under these conditions, the long-lived triplet state is the only energy storing species, and eq 4 can be rearranged to yield E_T. Using the values of α obtained from the plots in Figure 4b, and again recognizing that the exponential term in eq 4 reduces to 1 because $\tau_T \gg \tau_a$, a value of E_T for each ketone is readily obtained (Table 2). In this exercise, we used the average of Φ_Δ values shown in Table 2 as an estimate for Φ_T.

If one does not look too closely at cited errors, one might argue that the E_T value we obtain for PN, 181 ± 12 kJ/mol, is slightly lower than those obtained in previous studies; E_T = 186 ± 8 and 185 kJ/mol.[21,71] This observation may indicate a slight systematic error in our E_T determination. If so, then the E_T values listed for PD and BP may also be too small. Previously published correlations between values of E_T and the efficiency of singlet oxygen formation, S_Δ, for sensitizers with π,π^* triplet states[5] indeed suggest that our E_T values for PD and BP may be about 10 kJ/mol too low.

B. Two-Photon Properties.

To proceed with our investigation of PN, PD, and BP as versatile standard sensitizers for singlet oxygen generation, we conducted both experimental and computational studies of the two-photon absorption characteristics of these sensitizers. As outlined below, however, because two-photon transitions in PN are comparatively weak, the main focus of this investigation converged on PD and BP.

In a discussion of both one- and two-photon transition probabilities, it is pertinent to first consider the symmetries of the molecules involved. From calculated geometry optimizations, we ascertained that both PD and BP are indeed planar molecules, as intuitively expected from the nature of the aromatic π-system. Moreover, all calculated electronic states transform according to operations in the C_{2h} and C_s point groups for PD and BP, respectively. Both molecules exhibit a single well-defined ground state equilibrium geometry, with doubly occupied orbitals, giving rise to the ground state term configurations ^1A_g and $^1A'$ for PD and BP, respectively. As can be inferred from the structures in Chart 1, all of this also goes to say that PD is a centrosymmetric molecule (*i.e.*, contains a center of inversion), whereas BP is not centrosymmetric.

The issue of molecular symmetry is important with respect to selection rules that distinguish between one- and two-photon transitions.[55] Specifically, rules that derive from parity changes in the wavefunction dictate that, for a centrosymmetric molecule, a transition allowed as a two-photon process will be forbidden as a one-photon process, and *vice versa* (*i.e.*, states populated by two-photon absorption will not be populated by one-photon absorption, and *vice versa*).[55] Because PD is a centrosymmetric molecule, we thus expect to see a two-photon absorption spectrum that differs significantly from the corresponding one-photon spectrum. Conversely, for the noncentrosymmetric molecule BP, one would expect to see strong similarities between the one- and two-photon absorption spectra. (As a caveat to such generalized predictions, it is important to note that one- and two-photon transitions can be very close in energy. From an experimental perspective, distinguishing between such transitions can thus sometimes be difficult, particularly with femtosecond lasers that have a comparatively broad spectral profile.)

With these symmetry-based expectations in mind, we recorded two-photon excitation spectra for PD, BP, and PN in air-saturated toluene and quantified values of the two-photon absorption cross section, δ, for these molecules. In these experiments, where the photoproduced ketone triplet state is readily quenched by ground state oxygen (*vide supra*), we used the 1270 nm phosphorescence of singlet oxygen as a spectroscopic probe. Indeed, for a two-photon study of nonfluorescent molecules that also sensitize the production of singlet oxygen, this singlet-oxygen-based experimental approach to quantify δ has many desirable attributes.[7,8,10]

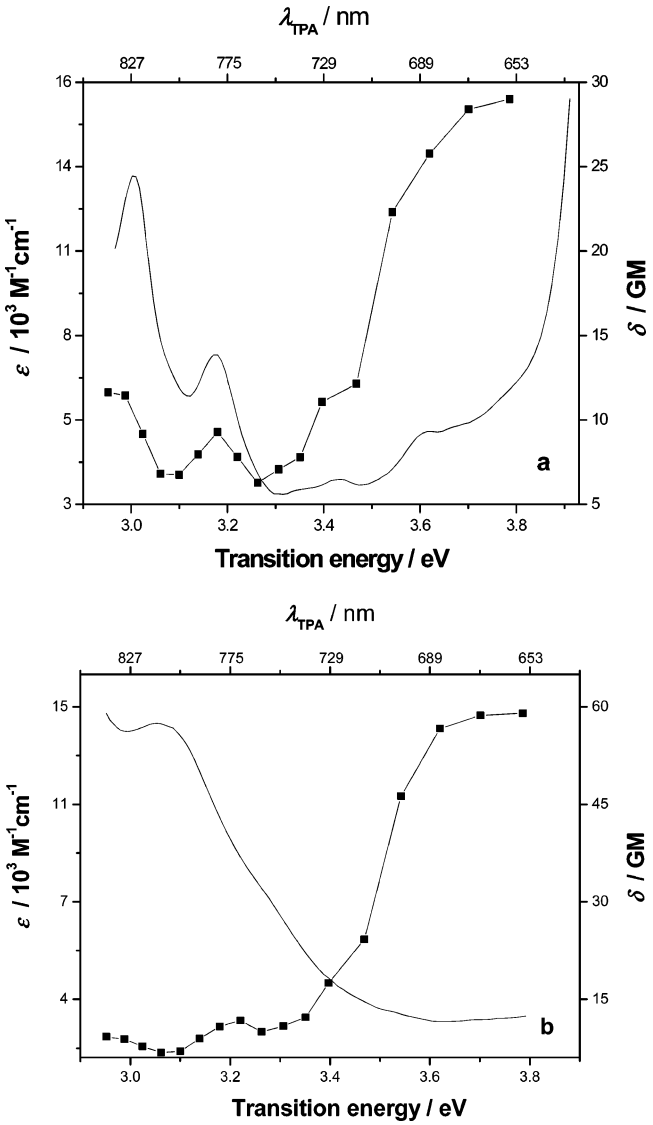

Figure 5. Two-photon excitation spectra (■, right side axes) and one-photon absorption spectra (—, left side axes), recorded in toluene, for BP (panel a) and PD (panel b). The two-photon spectra were obtained in an experiment relative to the standard molecule CNPhVB, and the estimated uncertainty on the individual data points is 15%. The wavelength scales shown on the upper *x*-axes refer only to the two-photon spectra, whereas the total transition energy refers equally to both one- and two-photon spectra.

At all excitation wavelengths used for the spectra that we report, we verified that the observed singlet oxygen signal scaled quadratically with incident laser power, as required for a two-photon process, and that the neat solvent gave no signal. Although irradiation of PD and BP gave strong signals that corresponded to comparatively large values of the two-photon absorption cross section (*vide infra*), data from PN only exhibited δ values below ~7 GM (see Supporting Information). Moreover, the two-photon study of PN was limited to the spectral range 685−740 nm because the singlet oxygen signal observed outside this range was either too weak to be accurately quantified or deviated from the required power-squared dependence.

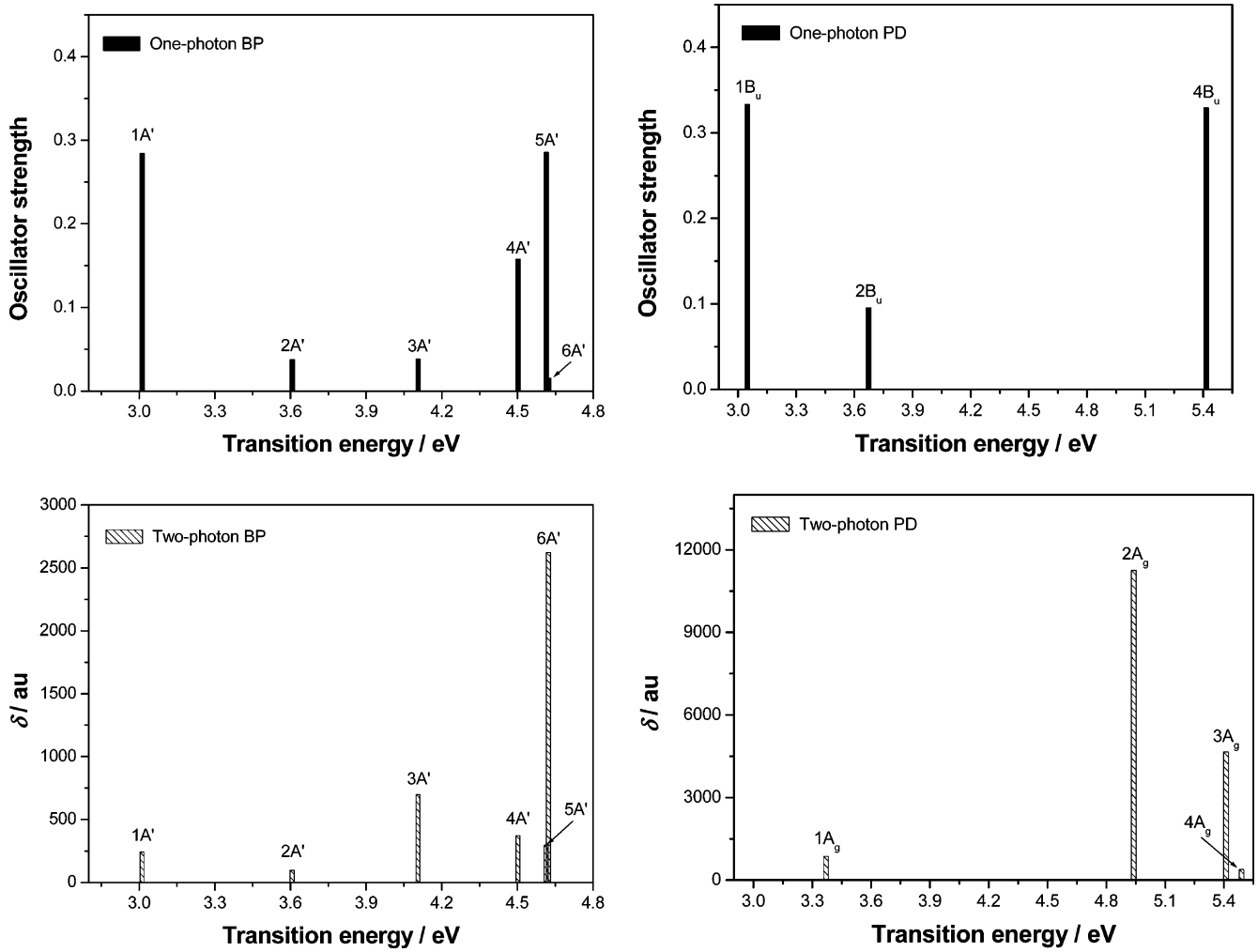

Figure 6. Results from density functional response theory computations on BP (left column) and PD (right column). The top row shows calculated one-photon transitions, and the bottom row shows calculated two-photon transitions.

Two-photon excitation spectra for PD and BP over the range 655−840 nm are shown in Figure 5. The data have been normalized to the standard CNPhVB, thus allowing us to plot the absorption cross section in GM units. At excitation wavelengths shorter than 655 nm, the singlet oxygen signals observed did not scale quadratically with the irradiation power indicating the possible onset of weak, but competing one-photon transitions. Also plotted in Figure 5 are the corresponding one-photon absorption spectra for PD and BP. Note that the pertinent *x*-axis scale used in this case is the total transition energy.

For the noncentrosymmetric molecule BP, there are clear similarities between the one- and two-photon spectra, just as expected (Figure 5a). On the other hand, and again as expected given the parity-based selection rules, the one- and two-photon spectra for the centrosymmetric molecule PD are effectively opposites of each other; a transition that is two-photon allowed is one-photon forbidden, and *vice versa* (Figure 5b). Thus, the absence or presence of molecular electronic symmetry is clearly evident in the spectra recorded for BP and PD, respectively.

The data in Figure 5 also reveal that both PD and BP have a comparatively large two-photon absorption band that appears to have a maximum around 650 nm. The two-photon absorption cross sections that we record for these molecules, both at 655 nm (Table 2) and at other wavelengths, are appreciable and certainly large enough for the efficient generation of detectable amounts of singlet oxygen.

To further address the issue of how symmetry is manifested in the absorption properties of PD and BP, and to complement the experimental data shown in Figure 5, we calculated one- and two-photon absorption spectra for both sensitizers. These computational results are summarized in Figure 6 and Table 3. Due to the principal limitation that our calculations represent gas-phase systems that lack solvent perturbations, we focus only on qualitative features of the respective spectra.

In the case of the noncentrosymmetric molecule BP, we can readily see from the results in Figure 6 and Table 3 that all the one-photon transitions are also allowed as two-photon transitions. Conversely, for the centrosymmetric molecule PD, the calculations show that a transition allowed as a one-photon process is forbidden as a two-photon process, and *vice versa.* Thus, these *ab initio* computational results clearly complement and support both our experimental results and the qualitative expectations derived from the parity-based selection rules. It is also reassuring to note that the computations reproduce the experimental observations that (1) the two-photon absorption cross sections for PD are, in general, larger than those for BP and (2) the two-photon absorption cross sections for PD and BP are larger than those for PN.

Conclusions

We have demonstrated that the aromatic ketones pyrene-1,6-dione, PD, and benzo[*cd*]pyren-5-one, BP, have many attributes

for use as sensitizer standards in either one- or two-photon photosensitized singlet oxygen experiments. Like the related aromatic ketone 1-phenalenone, PN, which is now widely accepted as a desirable one-photon singlet oxygen sensitizer standard, both PD and BP produce singlet oxygen with near unit quantum efficiency in both a polar (acetonitrile) as well as a nonpolar (toluene) solvent. However, with PD and BP, one can now use one-photon excitation wavelengths that are much longer than those used with PN. Furthermore, both PD and BP are much better two-photon singlet oxygen sensitizers than PN. This reflects the fact that the two-photon absorption cross sections for these more extensively conjugated molecules are significantly larger than those for PN over the wavelength range ~650−840 nm.

From a fundamental perspective, the one- and two-photon spectral data recorded on PD and BP provide a wonderful instructive example of the role that molecular symmetry plays in defining selection rules for the respective spectroscopic transitions. These data complement corresponding spectra recorded for the related hydrocarbon pyrene which also illustrate the influence of molecular symmetry.[72] Our data clearly show that for a noncentrosymmetric molecule, both one- and two-photon transitions to the same state are allowed. Our data also show that for a centrosymmetric molecule, transitions allowed as a one-photon process are forbidden as a two-photon process, and *vice versa*. These experimental results are complemented by the results of computations performed at a comparatively high level of theory.

We have further substantiated that the substituted phenylene vinylene CNPhVB is also a very useful standard reference molecule for two-photon experiments. It has a well-defined two-photon absorption spectrum over the range 625−900 nm, with comparatively large two-photon absorption cross sections. Moreover, it has the desirable attributes that it fluoresces ($\Phi_F = 0.86 \pm 0.07$[47]), sensitizes the production of singlet oxygen ($\Phi_\Delta = 0.11 \pm 0.02$[10]), and has an appreciable LIOAC signal,[10] and as such, it can be used as a standard in totally different experimental approaches to quantify two-photon absorption cross sections of a given molecule over a large spectral range. The principal disadvantage of CNPhVB is that it does not produce singlet oxygen in high yield and, for a singlet oxygen based experiment, it is here that the aromatic ketones PD and BP can be used to advantage.

Although the use of two-photon excitation has been wonderfully exploited for the creation of fluorescence-based images of a wide range of samples,[73,74] the creation of analogous two-photon sensitized $O_2(a^1\Delta_g) \rightarrow O_2(X^3\Sigma_g^-)$ phosphorescence-based singlet oxygen images of a sample is still in its infancy.[13−15] A key aspect of this latter field, particularly with respect to the imaging of biological samples, is the development and characterization of new two-photon singlet oxygen sensitizers. To this end, the standards described in this report should be of great use.

Acknowledgment. This work was supported by (1) the Danish National Research Foundation through a block grant for the Center for Oxygen Microscopy and Imaging and (2) the Danish Center for Scientific Computing.

Supporting Information Available: NMR spectra for BP, UV spectra for PD and PN in methanol, Cartesian coordinates for the ground state geometries of PN, PD, and BP used in the computations, the two-photon excitation spectrum of PN, calculated triplet state energies and orbital configurations for PD, PN, and BP, near IR phosphorescence data used to quantify singlet oxygen yields, and data from the control experiments using recrystallized PN. This material is available free of charge via the Internet at http://pubs.acs.org.

References and Notes

(1) Foote, C. S.; Clennan, E. L. In *Active Oxygen in Chemistry*; Foote, C. S., Valentine, J. S., Greenberg, A., Liebman, J. F., Eds.; Chapman and Hall: London, 1995; pp 105−140.

(2) Frimer, A. A., Ed. *Singlet Oxygen*; CRC Press: Boca Raton, FL, 1985; Vols. I−IV.

(3) Redmond, R. W.; Kochevar, I. E. *Photochem. Photobiol.* **2006**, *82*, 1178−1186.

(4) Dougherty, T. J.; Gomer, C. J.; Henderson, B. W.; Jori, G.; Kessel, D.; Korbelik, M.; Moan, J.; Peng, Q. *J. Natl. Cancer Inst.* **1998**, *90*, 889−905.

(5) Schweitzer, C.; Schmidt, R. *Chem. Rev.* **2003**, *103*, 1685−1757.

(6) Wilkinson, F.; Helman, W. P.; Ross, A. B. *J. Phys. Chem. Ref. Data* **1993**, *22*, 113−262.

(7) Frederiksen, P. K.; Jørgensen, M.; Ogilby, P. R. *J. Am. Chem. Soc.* **2001**, *123*, 1215−1221.

(8) Frederiksen, P. K.; McIlroy, S. P.; Nielsen, C. B.; Nikolajsen, L.; Skovsen, E.; Jørgensen, M.; Mikkelsen, K. V.; Ogilby, P. R. *J. Am. Chem. Soc.* **2005**, *127*, 255−269.

(9) Nielsen, C. B.; Johnsen, M.; Arnbjerg, J.; Pittelkow, M.; McIlroy, S. P.; Ogilby, P. R.; Jørgensen, M. *J. Org. Chem.* **2005**, *70*, 7065−7079.

(10) Arnbjerg, J.; Johnsen, M.; Frederiksen, P. K.; Braslavsky, S. E.; Ogilby, P. R. *J. Phys. Chem. A* **2006**, *110*, 7375−7385.

(11) Karotki, A.; Kruk, M.; Drobizhev, M.; Rebane, A.; Nickel, E.; Spangler, C. W. *IEEE J. Quantum Electron.* **2001**, *7*, 971−975.

(12) Oar, M. A.; Serin, J. M.; Dichtel, W. R.; Fréchet, J. M. J.; Ohulchanskyy, T. Y.; Prasad, P. N. *Chem. Mater.* **2005**, *17*, 2267−2275.

(13) Skovsen, E.; Snyder, J. W.; Ogilby, P. R. *Photochem. Photobiol.* **2006**, *82*, 1187−1197.

(14) Snyder, J. W.; Skovsen, E.; Lambert, J. D. C.; Poulsen, L.; Ogilby, P. R. *Phys. Chem. Chem. Phys.* **2006**, *8*, 4280−4293.

(15) Snyder, J. W.; Zebger, I.; Gao, Z.; Poulsen, L.; Frederiksen, P. K.; Skovsen, E.; McIlroy, S. P.; Klinger, M.; Andersen, L. K.; Ogilby, P. R. *Acc. Chem. Res.* **2004**, *37*, 894−901.

(16) McIlroy, S. P.; Cló, E.; Nikolajsen, L.; Frederiksen, P. K.; Nielsen, C. B.; Mikkelsen, K. V.; Gothelf, K. V.; Ogilby, P. R. *J. Org. Chem.* **2005**, *70*, 1134−1146.

(17) Arnbjerg, J.; Jiménez-Banzo, A.; Paterson, M. J.; Nonell, S.; Borrell, J. I.; Christiansen, O.; Ogilby, P. R. *J. Am. Chem. Soc.* **2007**, *129*, 5188−5199.

(18) Xu, C.; Webb, W. W. In *Topics in Fluorescence Spectroscopy*; Lakowicz, J., Ed.; Nonlinear and Two-Photon-Induced Fluorescence, Vol. 5; Plenum Press: New York, 1997; pp 471−540.

(19) Marti, C.; Jürgens, O.; Cuenca, O.; Casals, M.; Nonell, S. *J. Photochem. Photobiol., A. Chem.* **1996**, *97*, 11−18.

(20) Oliveros, E.; Suardi-Murasecco, P.; Aminian-Saghafi, T.; Braun, A. M. *Helv. Chim. Acta* **1991**, *74*, 79−90.

(21) Schmidt, R.; Tanielian, C.; Dunsbach, R.; Wolff, C. *J. Photochem. Photobiol., A: Chem.* **1994**, *79*, 11−17.

(22) Oliveros, E.; Bossmann, S. H.; Nonell, S.; Marti, C.; Heit, G.; Troscher, G.; Braun, A. M. *New J. Chem.* **1999**, *23*, 85−93.

(23) Rumi, M.; Ehrlich, J. E.; Heikal, A. A.; Perry, J. W.; Barlow, S.; Hu, Z.; McCord-Maughon, D.; Parker, T. C.; Röckel, H.; Thayumanavan, S.; Marder, S. R.; Beljonne, D.; Brédas, J.-L. *J. Am. Chem. Soc.* **2000**, *122*, 9500−9510.

(24) Strehmel, B.; Sarker, A. M.; Detert, H. *ChemPhysChem* **2003**, *4*, 249−259.

(25) Reinhardt, B. A.; Brott, L. L.; Clarson, S. J.; Dillard, A. G.; Bhatt, J. C.; Kannan, R.; Yuan, L.; He, G. S.; Prasad, P. N. *Chem. Mater.* **1998**, *10*, 1863−1874.

(26) Poulsen, T. D.; Frederiksen, P. K.; Jørgensen, M.; Mikkelsen, K. V.; Ogilby, P. R. *J. Phys. Chem. A* **2001**, *105*, 11488−11495.

(27) Norman, P.; Luo, Y.; Ågren, H. *J. Chem. Phys.* **1999**, *111*, 7758−7765.

(28) Wang, C.-K.; Macak, P.; Luo, Y.; Ågren, H. *J. Chem. Phys.* **2001**, *114*, 9813−9820.

(29) Olsen, J.; Jørgensen, P. *J. Chem. Phys.* **1985**, *82*, 3235−3264.

(30) Paterson, M. J.; Christiansen, O.; Jensen, F.; Ogilby, P. R. *Photochem. Photobiol.* **2006**, *82*, 1136−1160.

(31) Olsen, J.; Jørgensen, P. In *Modern Electronic Structure Theory, Part II. Advanced Series in Physical Chemistry*; Yarkony, D. R., Ed.; World Scientific: Singapore, 1995; pp 857−990.

(32) Christiansen, O.; Jørgensen, P.; Hättig, C. *Int. J. Quantum Chem.* **1998**, *68*, 1−52.

(33) Sasagane, K.; Aiga, F.; Itoh, R. *J. Chem. Phys.* **1993**, *99*, 3738−3778.

(34) Jonsson, D.; Vahtras, O.; Jansik, B.; Rinkevicius, Z.; Salek, P.; Ågren, H. In *Nonlinear Optical Properties of Matter: From Molecules to Condensed Phases*; Leszczynski, J., Ed.; Springer-Verlag: Berlin, 2006; pp 151−210.

(35) Christiansen, O.; Coriani, S.; Gauss, J.; Hättig, C.; Jørgensen, P.; Pawlowski, F.; Rizzo, A. In *Nonlinear Optical Properties of Matter: From Molecules to Condensed Phases*; Leszczynski, J., Ed.; Springer-Verlag: Berlin, 2006; pp 51−100.

(36) Paterson, M. J.; Christiansen, O.; Pawlowski, F.; Jørgensen, P.; Hättig, C.; Helgaker, T.; Salek, P. *J. Chem. Phys.* **2006**, *124*, 054322.

(37) Darmanyan, A. P. *Chem. Phys. Lett.* **1984**, *110*, 89−94.

(38) Grewer, C.; Wirp, C.; Neumann, M.; Brauer, H.-D. *Ber. Bunsen-Ges. Phys. Chem.* **1994**, *98*, 997−1003.

(39) Scurlock, R. D.; Nonell, S.; Braslavsky, S. E.; Ogilby, P. R. *J. Phys. Chem.* **1995**, *99*, 3521−3526.

(40) Braslavsky, S. E.; Heibel, G. E. *Chem. Rev.* **1992**, *92*, 1381−1410.

(41) Pineiro, M.; Carvalho, A. L.; Pereira, M. M.; Rocha-Gonsalves, A. M.; Arnaut, L. G.; Formosinho, S. J. *Chem. Eur. J.* **1998**, *4*, 2299−2307.

(42) Scurlock, R. D.; Ogilby, P. R. *J. Phys. Chem.* **1989**, *93*, 5493−5500.

(43) Pond, S. J. K.; Rumi, M.; Levin, M. D.; Parker, T. C.; Beljonne, D.; Day, M. W.; Brédas, J.-L.; Marder, S. R.; Perry, J. W. *J. Phys. Chem. A* **2002**, *106*, 11470−11480.

(44) Kennedy, S. M.; Lytle, F. E. *Anal. Chem.* **1986**, *58*, 2643−2647.

(45) Xu, C.; Webb, W. W. *J. Opt. Soc. Am., B* **1996**, *13*, 481−491.

(46) Sujatha, J.; Mishra, A. K. *J. Photochem. Photobiol, A: Chem.* **1996**, *101*, 245−250.

(47) Albota, M.; Beljonne, D.; Brédas, J.-L.; Ehrlich, J. E.; Fu, J.-Y.; Heikal, A. A.; Hess, S. E.; Kogej, T.; Levin, M. D.; Marder, S. R.; McCord-Maughon, D.; Perry, J. W.; Röckel, H.; Rumi, M.; Subramaniam, G.; Webb, W. W.; Wu, X.-L.; Xu, C. *Science* **1998**, *281*, 1653−1656.

(48) Fatiadi, A. J. *J. Chromatography* **1965**, *20*, 319−324.

(49) Reid, D. H.; Bonthrone, W. *J. Chem. Soc.* **1965**, 5920−5926.

(50) Frisch, M. J.; Trucks, G. W.; Schlegel, H. B.; Scuseria, G. E.; Robb, M. A.; Cheeseman, J. R.; Montgomery, J. A., Jr.; Vreven, T.; Kudin, K. N.; Burant, J. C.; Millam, J. M.; Iyengar, S. S.; Tomasi, J.; Barone, V.; Mennucci, B.; Cossi, M.; Scalmani, G.; Rega, N.; Petersson, G. A.; Nakatsuji, H.; Hada, M.; Ehara, M.; Toyota, K.; Fukuda, R.; Hasegawa, J.; Ishida, M.; Nakajima, T.; Honda, Y.; Kitao, O.; Nakai, H.; Klene, M.; Li, X.; Knox, J. E.; Hratchian, H. P.; Cross, J. B.; Bakken, V.; Adamo, C.; Jaramillo, J.; Gomperts, R.; Stratmann, R. E.; Yazyev, O.; Austin, A. J.; Cammi, R.; Pomelli, C.; Ochterski, J. W.; Ayala, P. Y.; Morokuma, K.; Voth, G. A.; Salvador, P.; Dannenberg, J. J.; Zakrzewski, V. G.; Dapprich, S.; Daniels, A. D.; Strain, M. C.; Farkas, O.; Malick, D. K.; Rabuck, A. D.; Raghavachari, K.; Foresman, J. B.; Ortiz, J. V.; Cui, Q.; Baboul, A. G.; Clifford, S.; Cioslowski, J.; Stefanov, B. B.; Liu, G.; Liashenko, A.; Piskorz, P.; Komaromi, I.; Martin, R. L.; Fox, D. J.; Keith, T.; Al-Laham, M. A.; Peng, C. Y.; Nanayakkara, A.; Challacombe, M.; Gill, P. M. W.; Johnson, B.; Chen, W.; Wong, M. W.; Gonzalez, C.; Pople, J. A. *Gaussian 03*, revision C.02; Gaussian Inc.: Wallingford, CT, 2004

(51) Helgaker, T.; Jensen, H. J. A.; Jørgensen, P.; Olsen, J.; Ruud, K.; Ågren, H.; Bak, K. L.; Bakken, V.; Christiansen, O.; Coriani, S.; Dahle, P.; Dalskov, E. K.; Enevoldsen, T.; Fernandez, B.; Hättig, C.; Hald, K.; Halkier, A.; Heiberg, H.; Hettema, H.; Jonsson, D.; Kirpekar, S.; Kobayashi, R.; Koch, H.; Mikkelsen, K. V.; Norman, P.; Packer, M. J.; Pedersen, T. B.; Ruden, T. A.; Sanchez, A.; Saue, T.; Sauer, S. P. A.; Schimmelpfennig, B.; Sylvester-Hvid, K. O.; Taylor, P. R.; Vahtras, O. *Dalton, a molecular electronic structure program*, release 2.0; 2005 (see http://www.kjemi.uio.no/software/dalton/dalton.html).

(52) Dreuw, A.; Head-Gordon, M. *Chem. Rev.* **2005**, *105*, 4009−4037.

(53) Birge, R. R.; Pierce, B. M. *J. Chem. Phys.* **1979**, *70*, 165−178.

(54) Masthay, M. B.; Findsen, L. A.; Pierce, B. M.; Bocian, D. F.; Lindsey, J. S.; Birge, R. R. *J. Chem. Phys.* **1986**, *84*, 3901−3915.

(55) McClain, W. M. *Acc. Chem. Res.* **1974**, *7*, 129−135.

(56) Shen, Y. R. *The Principles of Nonlinear Optics*; Wiley: New York, 1984.

(57) McClain, W. M. *J. Chem. Phys.* **1971**, *55*, 2789−2796.

(58) Kogej, T.; Beljonne, D.; Meyers, F.; Perry, J. W.; Marder, S. R.; Brédas, J. L. *Chem. Phys. Lett.* **1998**, *298*, 1−6.

(59) Rubio-Pons, O.; Luo, Y.; Ågren, H. *J. Chem. Phys.* **2006**, *124*, 094310.

(60) Paterson, M. J.; Kongsted, J.; Christiansen, O.; Mikkelsen, K. V.; Nielsen, C. B. *J. Chem. Phys.* **2006**, *125*, 184501.

(61) Jensen, F. *Introduction to Computational Chemistry, 2nd ed.*; John Wiley and Sons: Chichester, U.K., 2007.

(62) Koch, W.; Holthausen, M. C. *A Chemist's Guide to Density Functional Theory*; Wiley-VCH: Weinheim, 2001.

(63) Champagne, B.; Botek, E.; Nakano, M.; Nitta, T.; Yamaguchi, K. *J. Chem. Phys.* **2005**, *122*, 114315.

(64) Okutsu, T.; Noda, S.; Tanaka, S.; Kawai, A.; Obi, K.; Hiratsuka, H. *J. Photochem. Photobiol, A: Chem.* **2000**, *132*, 37−41.

(65) Wilkinson, F.; Helman, W. P.; Ross, A. B. *J. Phys. Chem. Ref. Data* **1995**, *24*, 663−1021.

(66) Gilbert, A.; Baggott, J. *Essentials of Molecular Photochemistry*; CRC Press: Boca Raton, FL, 1991.

(67) Peters, K. S.; Snyder, G. J. *Science* **1988**, *241*, 1053−1057.

(68) Gensch, T.; Viappiani, C.; Braslavsky, S. E. *J. Am. Chem. Soc.* **1999**, *121*, 10573−10582.

(69) Herbrich, R. P.; Schmidt, R. *J. Photochem. Photobiol, A: Chem.* **2000**, *133*, 149−158.

(70) Lower, S. K.; El-Sayed, M. A. *Chem. Rev.* **1966**, *66*, 199−241.

(71) Flors, C.; Nonell, S. *Helv. Chim. Acta* **2001**, *84*, 2533−2539.

(72) Salvi, P. R.; Foggi, P.; Castellucci, E. *Chem. Phys. Lett.* **1983**, *98*, 206−211.

(73) Denk, W.; Strickler, J. H.; Webb, W. W. *Science* **1990**, *248*, 73−76.

(74) Baumgart, T.; Hess, S. T.; Webb, W. W. *Nature* **2003**, *425*, 821−824.